Predictability of Boreal Forest Soil Bearing Capacity by Machine Learning

J. Pohjankukka[a,*], H. Riihimäki[b], P. Nevalainen[a], T. Pahikkala[a], J. Ala-Ilomäki[b], E. Hyvönen[c], J. Varjo[b], J. Heikkonen[a]

[a] *Department of Information Technology, University of Turku, FI-20014 Turku, Finland*
[b] *Natural Resources Institute Finland, FI-00790 Helsinki, Finland*
[c] *Geological Survey of Finland, FI-02151 Espoo, Finland*

Abstract

In forest harvesting, terrain trafficability is the key parameter needed for route planning. Advance knowledge of the soil bearing capacity is crucial for heavy machinery operations. Especially peatland areas can cause severe problems for harvesting operations and can result in increased costs. In addition to avoiding potential damage to the soil, route planning must also take into consideration the root damage to the remaining trees. In this paper we study the predictability of boreal soil load bearing capacity by using remote sensing data and field measurement data. We conduct our research by using both linear and nonlinear methods of machine learning. With the best prediction method, ridge regression, the results are promising with a C-index value higher than 0.68 up to 200 meter prediction range from the closest point with known bearing capacity, the baseline value being 0.5. The load bearing classification of the soil resulted in 76% accuracy up to 60 meters by using a multilayer perceptron method. The results indicate that there is a potential for production applications and that there is a great need for automatic real-time sensoring in order to produce applicable predictions.

Keywords: Terrain trafficability, Soil bearing capacity prediction, Forest harvesting, Machine learning, Open data

1. Introduction

Terrain trafficability in forests is currently one of the most important issues in boreal timber harvesting. Conducting harvesting operations during good soil bearing conditions is crucial since improperly timed operations can cause serious economical and ecological damage. Vehicular loading exceeding soil strength causes not only soil damage, but also damage to trees, mostly to the tree roots, but sometimes to tree stem as well due to increasing uncontrolled motion of the forwarder.

Damage to roots and stems can lead to fungal infection which eventually causes wood discoloration and in the worst case decay. In addition, the water and nutrition conditions of the forest soil can change as a result of soil settling [1]. The operation of forest machines is therefore avoided during

*Corresponding author, Tel.: +358 50522 1551
Email address: jonne.pohjankukka@utu.fi (J. Pohjankukka)

the period of high soil failure risk and the harvesting is postponed to the winter when soil is normally frozen. It is estimated that the seasonal variation in timber procurement causes approximately 100 M € costs in Finland alone [2]. In addition, operations in poorly bearing conditions increase time and fuel consumption and decrease the efficiency of harvesting operations [3].

Furthermore, deep ruts caused by forwarding affect the general acceptability of the forest operations. The costs caused by challenging trafficability conditions could be decreased by additional information on soil conditions, especially soil bearing capacity. The load bearing capacity of soil is often described by its penetration resistance. Accordingly, forest operations could be planned to be performed during adequate bearing capacity or routed to avoid sections of poor bearing capacity, thus minimizing the damage and maximizing the efficiency of harvesting.

In this study we conduct a research on the prediction of soil bearing capacity by using remote sensing and field measurement data. We have analysed two cases, firstly visual soil damage classification and secondly soil penetration resistance prediction. The data sets are provided by Natural Resources Institute Finland (LUKE), Metsäteho Ltd., the Geological Survey of Finland (GTK), National Land Survey of Finland (NLS) and Finnish Meteorological Institute (FMI). Similar studies have been conducted in [4; 5] where soil properties such as type and water permeability was estimated in order to have predictions on the soil bearing capacity using public data. Related studies have been conducted in [6] where soil respiration rates are predicted from temperature, moisture content and soil type and [7], where the soil type in desert landscapes was predicted using classification tree analysis.

2. Background

Timber harvesting systems vary across the world. In Finland, the mechanized cut-to-length harvesting system is utilized almost exclusively [8]. Harvesting operations in Finland are typically commercial thinnings or clear cuttings. In a traditional thinning operation only a part of the trees, on average 30%, are cut, leaving most of the trees standing [9]. Depending on stand properties thinnings are typically done one to three times during the rotation of a stand [9].

The rotation period of a stand usually ends to a final felling, where all trees of commercial value are cut. Some individual tree clusters are left standing for example to retain biodiversity [10]. The structure of private forest ownership in Finland has changed, which is causing pressure to change the forestry practices, as many forest owners are no more dependent of forest income and emphasize multiple values in management decisions. The commercial aspect of harvesting has become less pronounced, while environmental standpoint has gained more attention. More than a half of the forest owners are satisfied with the current forest management practices, where every sixth forest owner feels unsatisfied especially with clear cuttings, lack of management alternatives, soil preparation and damage caused by heavy machinery [11]. So far the use of alternative forest management methods including selection cuttings has been marginal con-

centrating on urban forests, landscape protection areas, valuable habitats, riparian and other buffer zones. If uneven-aged forest management becomes more popular in future, it increases the amount of thinnings. Uneven-aged thinnings place even more challenges to harvesting machinery in respect to avoiding damages and risk of root rot.

3. Research area and data sets

3.1. Research area

The data sets were collected from various locations around the area of Pieksämäki, a municipality located in the province of Eastern Finland 62°18'N 27°08'E. The research areas were divided into two cases based on the response variable. The predictor data sets varied between the two cases as illustrated in tables 1 and 2.

3.2. Multi-Source National Forest Inventory data

The Multi-Source National Forest Inventory (MS-NFI) holds the state of Finnish forests in high spatial resolution (20 m). The data is updated every second year. The parameters are derived by generalizing the field measured sample plot data applying mainly Landsat imagery and KNN method as well as digital map information. 43 numerical features include information regarding, for example, biomass and volume of growing stock and site type. These multi-source features exhibit built-in dependencies, thus the final number of useful features is lower. An excellent, detailed description regarding the MS-NFI is given by [12].

3.3. Digital Elevation Model data

We downloaded digital elevation model (DEM) data from the file service for open data by the National Land Survey of Finland. The DEM was made from airborne laser scanning data with the resolution of at least 0.5 samples/m^2, which is equivalent to approximately 1.4 m distance between samples. The grid size of the DEM data set was 2 m. Several geomorphometric variables were derived from the NLS DEM in SAGA GIS environment. In our analysis we used the geomorphometric features: plan curvature, profile curvature, slope, topographic wetness index, flow area, aspect, diffuse insolation and direct insolation [13; 14; 15; 16; 17]. These derived features are more efficient for prediction than raw height data alone.

3.4. Weather data

Weather data consisting of temperature (°C) and rainfall (mm) for years 2011-2013 was provided by the Finnish Meteorological Institute. The grid size of the data set was 10 km. In our analyses we used the mean temperature and rainfall of the last 30 days as predictor features for each observation of the response value. For example if an observation of the response value was measured June 15, 2013 the mean temperature and rainfall predictor features for the response value observation were calculated from the time interval May 16 - June 14, 2013.

3.5. Aerial Gamma-ray Spectroscopy data

The aerial gamma-ray data with grid size of 50 m was provided by the Geological Survey of Finland (GTK). The raster data is based on gamma-ray flux from potassium, which is the decay process

Table 1: Predictor data sets used in prediction of soil damage response variable. RS stands for remote sensing data and FM stands for field measurement data

Data set	**Type**	**Grid size**
Digital Elevation Model data	RS	2 m
Multi-source National Forest Inventory data	RS	20 m
Soil type data	RS	20 m
Peatland data	RS	20 m
Gamma-ray spectroscopy data	RS	50 m
Weather data	RS	10 km

Table 2: Predictor data sets used in prediction of penetration resistance response variable.

Data set	**Type**	**Grid size**
Stoniness data	FM	2 m
Peatland data	FM	2 m
Soil moisture data	FM	2 m
Digital Elevation Model data	RS	2 m
Multi-source National Forest Inventory data	RS	20 m
Weather data	RS	10 km

of the naturally occurring chemical element potassium (K). This data indicates many significant characteristics of the soil, including the tendency to stay moist after precipitation and tendency to frost heaving [18]. Also the soil type, especially density, porosity, grain size and humidity of the soil have an effect on gamma-ray radiation. Areas with high gamma-radiation tend to have lower soil moisture and vice versa. We derived several statistical and textural features from Gamma-ray data such as: 3×3 windowed mean, 3×3 windowed standard deviation, Gabor filter features (see e.g. 19) and Local Binary Pattern features [20].

3.6. Peatland data

The peatland data was compiled by LUKE using the open geographic information data derived from NLS Topographic database [21] depicting the terrain and covering the whole of Finland. The positional accuracy of the NSL Topographic database corresponds to that of scales 1:5000 - 1:10000 [21]. The peatland mask consist of four different NLS Topographic database elements depicting different type of peatlands. These elements were first combined and then rasterized to 20 m grid using ArcMap software [22]. The definitions for peatlands in the NLS Topograhic database are: 1) area is mostly

covered by peatland vegetation and 2) a minimum of 0.3 m peat thickness [21]. A minimum criteria for area is 1000 m^2. Area with peat thickness less than 0.3 m can also be classified as peatland if it is covered by peatland vegetation.

3.7. Subsoil and topsoil data

GTK provided the analysis of subsoil classification data and topsoil classification data from Pieksämäki target area. The soil type data is represented by positive integer values, which indicate the pre-classified soil types. Both of the soil type data sets consisted of twelve distinct soil types e.g. bedrock, *Sphagnum* peat, *Carex* peat and sandy till. The grid size of these data sets were also 20 m.

3.8. Soil moisture data

Gravimetric soil water content was measured from the samples by drying the soil samples and calculating the weight difference of dry and wet soil sample [23].

3.9. Soil damage data

Approximately 36 km of strip roads were walked through and visually assessed into damage classes by a forest operations expert. The data was kindly provided to us by Metsäteho Ltd. in 2013. The soil damage data was classified into three main ordinal classes based on the rut depth caused by forest harvesting machinery. The three classes were: 1) No damage; 2) Slight damage; and 3) Damage[1].

[1]Includes strip road sections covered by brash mat, originally classified as "potential damage", since without brash mat they likely would have been damaged.

The original dataset required preprocessing since the field recorded GPS-tracks included locational errors (zig-zag -motion). After the data was preprocessed to produce a smooth line form, we converted strip road lines into points and extracted values from selected features, e.g. MS-NFI and topographic variables.

3.10. Soil penetration resistance, stoniness and shear modulus

The total of 50 penetration resistance measurements were taken on two different locations in Kumpunen, Pieksämäki, Finland (N 6921354, E 501297 in ETRS-TM35FIN coordinates). The study was conducted during a commercial thinning operation. The plot locations were selected based on expert judgment to cover the gradient between dry mineral soil with high bearing capacity and wet organic soil with low bearing capacity. 15 plots were measured from dry site and 35 plots were measured from wetter, partly paludificated site. Sites were located roughly 490 m meters apart from each other. Depth of organic soil varied from 0 to almost 90 cm. We measured the soil penetration resistance using a penetrometer [24] at five different locations around and between the wheel tracks to avoid the random effect caused by e.g. hitting a tree root in a single measurement. This method is illustrated in figure 1. Shear modulus was measured at the same locations with a spiked shear vane [25]. The accumulation of logging residue significantly hindered measuring, and it was not always possible to place measurements systematically.

3.11. Rut depth measurement

Depth of both wheel ruts was measured using an inversed U-shaped frame with its feet resting on the undeformed soil surface outside wheel rut, which formed the reference level. Individual observations were averaged to plot level. First measurements were taken after the harvester and the rut formation was measured again after each pass of the forwarder collecting the timber from the cutting area. The extraction road was cleared of logging residue after the harvester pass in order to observe the effect of soil properties on forwarder rut formation without the reinforcing effect of brash [3]. The accumulated mass traversed over each measuring location was defined as the sum of net vehicle mass plus the mass of load for all the passes [3].

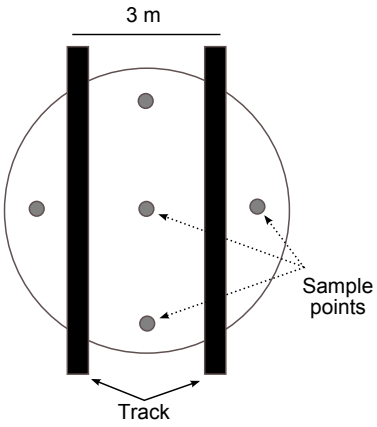

Figure 1: Illustration of how the field measurements were made. Black rectangles represent the wheel tracks and gray points represent the measurement points. The width of the track was approximately 0.4 m and distance from the center of the left track to the center of the right track was 2.8 m.

4. Methods

The possibilities to predict the response variables were estimated using both linear and non-linear methods. Next we will describe the used prediction methods including leave-one-out cross-validation with a dead zone approach for the model performance estimation given by the concordance index (C-index).

4.1. Leave-one-out cross-validation with a dead zone

In geographical applications there is bound to be some sort of spatial autocorrelation between the data points. Data points very close to each other geographically have intuitively larger spatial autocorrelation than data points far apart. Accordingly, using the traditional cross-validation approach (see e.g. 26) that assumes the mutual independence of the data points, is not suitable here, as it only estimates the prediction capability of individual test data points, regardless of their distance from the training data. We need a way of simulating the predictions in a practical situation which is why we use the so-called *leave-one-out cross-validation with a dead zone* (LOOCVDZ), [5].

The idea of the LOOCVDZ method is to simulate the prediction capability of the model in such a situation, where the point for which the prediction is to be made is at least n meters away from the closest training point. For each data point at a time, we create a perimeter (dead zone) of radius δ around the point and remove from the training data all the points falling inside the perimeter including the test point itself. A model is trained with the reduced training data set and a prediction is performed for the test point with the learned model. This process is repeated over the whole data set, just like an ordinary leave-one-out cross-validation.

The LOOCVDZ method gives us a way of simulating a harvester or a forwarder predicting soil bearing capacity, when the closest known measurements are at least n meters away. In figure 2 we have illustrated the LOOCVDZ method.

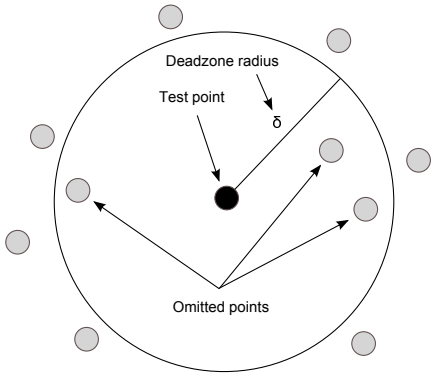

Figure 2: Illustration of the dead zone with perimeter determined by δ. The black point is the one whose label we aim to predict. The data inside the dead zone will be omitted from training the model used to predict the label of the test point.

4.2. Concordance index

Concordance index (C-index) was the main performance measure used in the analyses [27]. Concordance index measures the relative ranking of paired data points in the sets $V = \{y_1, ..., y_n\}$ and $P = \{\hat{y}_1, ..., \hat{y}_n\}$, where V is the set of observed labels and P is the corresponding set of predictions. The C-index measures how well the prediction model was able to rank the predictions into correct order. It is a particularly useful measure in situations where we are not especially interested in the absolute accuracy of the prediction value, but rather where we need to make a choice between a set of alternatives. In our application we are interested in selecting the most supporting area or route from a set of alternatives for the forest machine. Explicitly concordance index is defined as:

$$\text{C-index} = \frac{1}{N} \sum_{y_i < y_j} h\left(\hat{y}_i - \hat{y}_j\right), \tag{1}$$

where $N = |\{\ (i,j) \mid y_i < y_j\ \}|$ is the normalization constant which equals to the number of data pairs with different label values and $h(u)$ is the step function returning $1.0, 0.5$ and 0.0 for $u < 0, u = 0$ and $u > 0$, respectively. The further apart from 0.5 C-index is, the better the model was able to capture the pattern in the data.

4.3. Ridge regression

Ridge regression, also known as Tikhonov regularization [28] is the regularized version of the standard linear regression. Let $\mathbf{x}_i \in \mathbb{R}^p$ be the feature vector of the ith sample point, $\mathbf{w} \in \mathbb{R}^p$ is a vector of weights and $y_i \in \mathbb{R}$ is the response value of ith sample. In ridge regression our task is to find the set of weights $\mathbf{w}$, such that the objective function:

$$E(\mathbf{w}) = \frac{1}{n} \sum_{i=1}^{n} \left(\mathbf{x}_i^T \mathbf{w} - y_i\right) + \frac{\lambda}{n} \mathbf{w}^T \mathbf{w}, \tag{2}$$

is minimized. In 2, $n \in \mathbb{N}$ is the number of data points and $\lambda > 0$ is the regularization parameter.

4.4. Multilayer perceptron

Multilayer perceptron (MLP) is a feedforward neural network [29; 30], where we try to minimize the objective function:

$$E(\mathbf{w}) = \frac{1}{n} \sum_{i=1}^{n} \left(y_i - a(\mathbf{x}_i, \mathbf{w})\right)^2, \tag{3}$$

where $\mathbf{w}$ is the set of weights of the network, a_i is the ith activation of the output node given input

$\mathbf{x}_i \in \mathbb{R}^p$ and $y_i \in \mathbb{R}$ is the corresponding response value. The set of weights $\mathbf{w}$ is defined as:

$$\mathbf{w} := \left\{ w_{ij}^{(l)} \;\middle|\; 1 \leq l \leq L, 0 \leq i \leq d^{(l-1)}, 1 \leq j \leq d^{(l)} \right\},$$

where L is the number of hidden layers and $d^{(l)}$ is the number of hidden nodes on layer l. The activation functions in the hidden nodes are $\tanh(\mathbf{x})$ functions and the output activation function was selected to be a linear function.

A popular regularization approach for MLPs is to construct a committee of MLP networks trained with early stop training [29] in which training data are divided into two parts. The first part is used to train the MLP and the other part is used to monitor the validation error. Training is stopped when the validation error begins to increase. This random splitting scenario is repeated for all committee members and the final output of the MLP committee is obtained by counting the average output of the committee members. Early stop is an *ad hoc* method for regularization, but it is simple, fast and in many cases gives good results. We used a MLP early stop committee (MLP-ESC) of 10 networks with 10 hidden units.

4.5. k-nearest neighbor

k-nearest neighbor [31] is the simplest of the used methods, but still a powerful nonlinear method for many applications. In k-nearest neighbor we predict the label $\hat{y}_i$ of a test point $\mathbf{x}_i \in \mathbb{R}^p$ by taking the average value of the labels of its k nearest neighbors, i.e. we use the formula:

$$\hat{y}_i = \frac{1}{k} \sum_{j=1}^{k} y_j,$$

where the values $y_j \in \mathbb{R}$, $i = 1, ..., k$ are the labels of the points $\mathbf{x}_j$ that are closest to the test point $\mathbf{x}_i$. Euclidian distance is the standard metric used in this method for finding the closest neighbors.

5. Analysis and results

We have separated our analysis into two cases based on the response variables:

- Case 1: Soil damage prediction
- Case 2: Soil penetration resistance prediction

Both of these variables can be used as indicators for soil load bearing capacity.

5.1. Case 1: Soil damage prediction

In soil damage prediction our data set consisted of 11795 points from harvesting operations including both thinning and clearcutting. The predictor variables consisted from various remote sensing data sets and their derived features, totaling to 83 variables used in the analysis. The target variable for prediction was soil damage class consisting of three ordinal damage classes (no damage, slight damage, damage). The used data sets in this case are listed in table 1.

We tried two different approaches in predicting soil damage class, firstly predicting the soil damage variable without any modifications to the label values and, secondly, combining the damage classes 'slight damage' and 'damage' into one class so that we could get a binary prediction problem (no damage - damage). The purpose of this second approach was to detect whether the prediction model is able to distinguish between non-damaged and damaged

soil points. The multilayer perceptron model was trained with 11295 data points and tested with a sample of 500 data points, because the overall calculations using LOOCVDZ would have taken far too much time using the entire data set. We have illustrated the prediction results using LOOCVDZ for these two approaches in figure 3.

In both cases the results indicate that a moderate prediction performance to a 20-30 meters range is reached especially with k-nearest neighbor and ridge regression. Ridge regression stays above baseline up to 200 meters but has nonetheless poor performance. Low prediction performance in case 1 was expected due to low quality of the provided response variable. Poor results of the analysis based on visually classified data implicated the need for physical measurements. It was concluded that more accurate measurements were needed in order to improve the performance of the models. This insight motivated the collection of new data, i.e. penetration resistance as response variable.

5.2. Case 2: Soil penetration resistance prediction

Due to high noisiness of the response variable, the soil damage prediction resulted in maximum of 20-30 meter moderate prediction performance. This problem was tackled in the case of soil penetration resistance prediction, where an accurate data set, measured with an electrically driven and recording penetrometer, was provided by LUKE. The penetrometer proved superior over the spiked shear vane in varying mineral soil peatland conditions. The results of this experiment indicated the need for real-time automatic sensors for harvesters in order to produce sufficiently accurate input data to produce applicable prediction rates. A total of 50 penetration resistance profiles were collected from two test sites. The test sites were selected to have differing properties in terms of penetration resistance. The first site was located on mineral soil with good bearing capacity, whereas the second was partly covered by a layer of peat. Based on physical measurements, the quality of the data was much higher than that of the soil damage data. We have listed the used data sets for this case in table 2. In the analysis, the predictor data sets consisted of 50 variables. Also in this case we divided the prediction of soil penetration resistance into two approaches. In the first approach we implemented a regression model for the penetration resistance variable. In the second approach we divided the data into two classes based on the following criterion:

$$\text{Class of data point } \mathbf{x}_i = \begin{cases} 1 & \text{if } y_i \geq 5000 \text{ kPa} \\ 0 & \text{if } y_i < 5000 \text{ kPa} \end{cases},$$

where $\mathbf{x}_i$ is the ith data point with elements corresponding to feature values and y_i is the corresponding value of penetration resistance for that point. In this case the problem was to classify a data point $\mathbf{x}_i$ either into class 1 or 0. We have illustrated the results for both of these approaches in figure 4. We can notice that the results are much better than in it was in case 1. C-index stays above 0.6 up to 100 meters for multilayer perceptron and ridge regression. Ridge regression stays above 0.6 up to 200 meters. In classification case we got 66% classification accuracy up to 100 meters by MLP and almost 70% accuracy up to 40 meters by MLP-ESC.

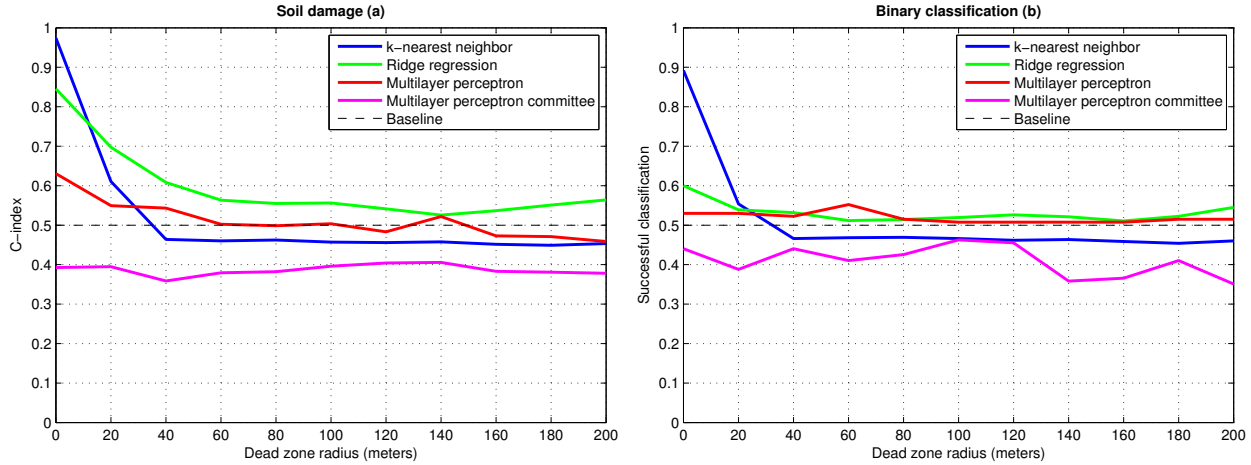

Figure 3: Prediction results for case 1: soil damage class (a) and binary classification (b). The results show that there is a moderate prediction accuracy up to 20 meters in both regression and classification. k-nearest neighbor achieves the highest performance to 20 meter range. Ridge regression gives highest results after 20 meters.

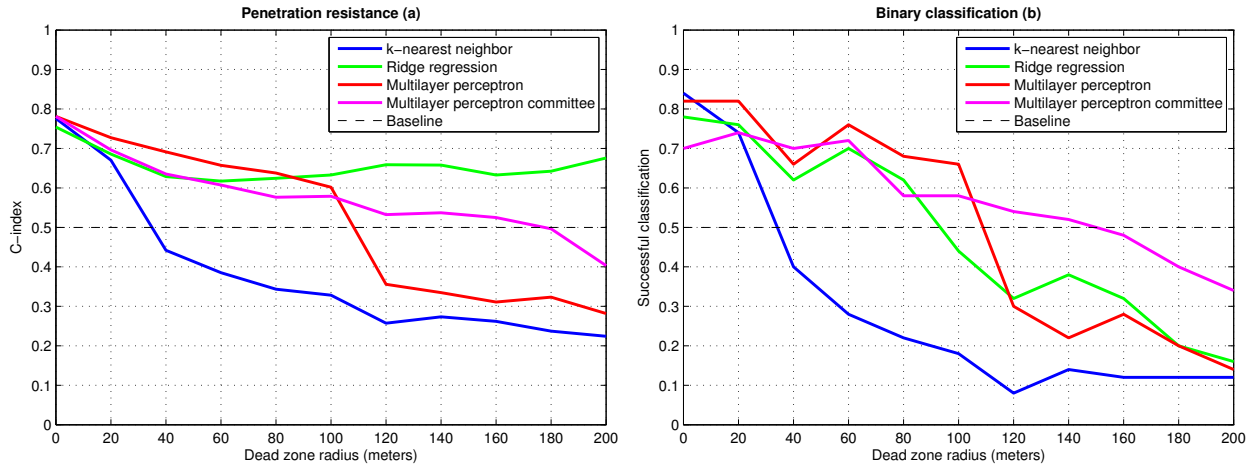

Figure 4: Prediction results for case 2: soil penetration resistance (a) and soil bearing capacity binary classification (b). Ridge regression and multilayer perceptron achieve the highest results up to 100 meter range. For multilayer perceptron (MLP) we have more than 70% classification accuracy up to 40 meter range.

6. Conclusion

The results indicated moderate prediction rates up to 20 meters for the soil damage regression case. After 20 meters the prediction performance drops dramatically and a random yes/no guess produces better results. C-index value stays just above the baseline 0.5 up to 200 meters for the ridge regression model. In the soil damage classification case we achieved more than 60% classification rate up to 20 meters as well. We therefore conclude that more precise measurements are needed for modelling purposes. In the case of penetration resistance prediction we achieved a C-index higher than 0.6 up to 200 meters for ridge regression model. With soil bearing capacity classification we achieved more than 66% successful classification up to 100 meters by MLP. Up to 20 meters we achieved classification accuracy of more than 80% also by MLP. The better results in the case of penetration resistance data is explained by the higher quality of the used data sets because the data samples were based on physical measurements.

As a summary of the results, in case 1; the soil damage prediction remains moderate up to 20 meters after which the result drop close to baseline value. In case 2; the soil penetration resistance prediction the results remain very good up to 20 meters, good up to 100 meters after which the results start to drop below baseline. It was evident that the used data sets in penetration resistance case was more reliable and contained less noise than the data sets used in soil damage case. This points out the necessity of accurate and real-time measurements in order to produce applicable forecast models for harvesting operations. If the data quality is not high enough the prediction performance deteriorates rapidly. However the measured data sets were rather small, which suggests further analysis in more varied environments in the future.

We conclude, that more detailed field data is required, i.e. physical measurements and detailed information about the motions of the machinery within the stand, since for example the accumulation of traversed mass over each location is one of the main variables explaining soil damages [3]. These can be achieved through online learning based on trafficability data accumulated by harvesters or other field studies. Vertical distance to drainage network should also be tested [32]. Further validation with weather data and water budget models should be continued in the future as it is one of the key variables affecting trafficability of fine grained mineral and organic soils.

Acknowledgments

The study was carried out in *New Computational Methods for Effective Utilization of Public Data* (ULJATH)-project funded by the Finnish Funding Agency for Innovation (TEKES).

References

[1] E. Ring, S. Löfgren, I. Bergkvist, L. Högbom, Många bäckar små..., Tech. Rep. 2, Skogforsk (2006).

[2] O. Pennanen, O. Mäkelä, Raakapuukuljetusten kelirikkohaittojen vähentäminen, Metsätehon raportti, Tech. Rep. 153, Metsäteho Ltd. (2003).

[3] M. Sirén, J. Ala-Ilomäki, H. Mäkinen, S. Lamminen, T. Mikkola, Harvesting damage caused by thinning of norway spruce in unfrozen soil, International Journal of Forest Engineering 24 (1) (2013) 60–75.

[4] J. Pohjankukka, P. Nevalainen, T. Pahikkala, E. Hyvönen, R. Sutinen, P. Hänninen, J. Heikkonen, Arctic soil hydraulic conductivity and soil type recognition based on aerial gamma-ray spectroscopy and topographical data, in: M. Borga, A. Heyden, D. Laurendeau, M. Felsberg, K. Boyer (Eds.), Proceedings of the 22nd International Conference on Pattern Recognition (ICPR 2014), IEEE, 2014, pp. 1822–1827.

[5] J. Pohjankukka, P. Nevalainen, T. Pahikkala, E. Hyvönen, M. Middleton, P. Hänninen, J. Ala-Ilomäki, J. Heikkonen, Predicting water permeability of the soil based on open data, in: L. Iliadis, I. Maglogiannis, H. Papadopoulos (Eds.), Proceedings of the 10th International Conference on Artificial Intelligence Applications and Innovations (AIAI 2014), Vol. 436 of IFIP Advances in Information and Communication Technology, Springer, 2014, pp. 436–446.

[6] A. Azzalini, P. Diggle, Prediction of soil respiration rates from temperature, moisture and soil type, Journal of the Royal Statistical Society - Series C: Applied Statistics 43 (3) (1994) 505–526.

[7] R. Schulte, J. Diamond, K. Finkele, N. Holden, A. Brereton, Predicting the soil moisture conditions of irish grasslands, Irish Journal of Agricultural and Food Research 44 (2005) 95–110.

[8] J. Uusitalo, Introduction to Forest Operations and Technology, Vol. 1, Metsäkustannus Ltd, 2010.

[9] O. Äijälä, A. Koistinen, J. Sved, K. Vanhatalo, P. Väisänen, Tapio - Hyvän metsänhoidon suositukset: Forest Management Practice Recommendations, Vol. 1, Metsäkustannus Ltd, 2014.

[10] L. Gustafsson, K. Perhans, Biodiversity conservation in swedish forests: Ways forward for a 30-year-old multi-scaled approach, AMBIO: A Journal of the Human Environment 39 (8) (2010) 546–554.

[11] H. Hänninen, H. Karppinen, Metsänomistusrakenteen muutos ja puuntarjonta: Change in forest ownership and wood supply, finnish forest sector economic outlook, Tech. rep., Finnish Forest Research Institute (2010).

[12] E. Tomppo, M. Katila, K. Mäkisara, J. Peräsaari, Multi-source national forest inventory methods and applications, Vol. 18 of Managing Forest Ecosystems, Springer, 2008.

[13] L. Zevenbergen, C. Thorne, Quantitative analysis of land surface topography, Earth Surface Processes and Landforms 12 (1) (1987) 47–56.

[14] J. Wood, Geomorphometry in landserf, in: T. Hengl, H. Reuter (Eds.), Developments in Soil Science, Vol. 33, 12, 2009, pp. 333–349.

[15] J. Wood, The geomorphological characterisation of digital elevation models, Ph.D. thesis, University of Leicester (1996).

[16] K. Beven, M. Kirkby, A physically based, variable contributing area model of basin hydrology, Hydrological Sciences Bulletin 24 (1) (1979) 43–69.

[17] J. Seibert, B. McGlynn, A new triangular multiple flow direction algorithm for computing upslope areas from gridded digital elevation models, Water Resources Research 43 (4) (2007) na–na, w04501.

[18] E. Hyvönen, M. Pänttäjä, M.-L. Sutinen, R. Sutinen, Assessing site suitability for scots pine using airborne and terrestrial gamma-ray measurements in finnish lapland, Canadian Journal of Forest Research 33 (5) (2003) 796–806.

[19] H. Feichtinger, T. Strohmer, Gabor Analysis and Algorithms: Theory and Applications, Birkhäuser, 1997.

[20] M. Pietikäinen, A. Hadid, G. Zhao, T. Ahonen, Computer Vision Using Local Binary Patterns, Computational Imaging and Vision, Springer, 2011.

[21] NLS, NLS Topographic database, National Land Survey of Finland (2014).
URL http://www.maanmittauslaitos.fi/en/opendata

[22] ArcMap, ArcGIS Platform, ESRI (2014).
URL http://www.esri.com/software/arcgis

[23] ASTM D2216-10, Standard Test Methods for Laboratory Determination of Water (Moisture) Content of Soil and Rock by Mass, ASTM International, West Conshohocken, PA (2010).

[24] T. Muro, O'Brien, Terramechanics: Land Locomotion Mechanics, CRC Press, 2004.

[25] J. Ala-Ilomäki, Spiked shear vane - a new tool for measuring peatland top layer strength, Mires and Peat 64 (2–3) (2013) 113–118.

[26] Y. Abu-Mostafa, M. Magdon-Ismail, H. Lin, Learning from data, Vol. 1, AMLBook, 2012.

[27] M. Gönen, G. Heller, Concordance probability and discriminatory power in proportional hazards regression, Biometrika 92 (4) (2005) 965–970.

[28] V. Vapnik, Statistical Learning Theory, Vol. 1, Wiley-Interscience, 1998.

[29] C. Bishop, Neural Networks for Pattern Recognition, Oxford University Press, 1996.

[30] I. Nabney, NETLAB: Algorithms for Pattern Recognition, no. 1, Springer, 2004.

[31] T. Cover, P. Hart, Nearest neighbor pattern classification, IEEE Transactions on Information Theory 13 (1) (1967) 21–27.

[32] P. Murphy, J. Ogilvie, P. Arp, Topographic modelling of soil moisture conditions: a comparison and verification of two models, European Journal of Soil Science 60 (1) (2009) 94–109.